World Academy of Science, Engineering and Technology
International Journal of Electrical and Computer Engineering
Vol:7, No:4, 2013

Thermal Analysis of a Sliding Electric Contact System Using Finite Element Method

Adrian T. Pleşca

***Abstract*—**In this paper a three dimensional thermal model of a sliding contact system is proposed for both steady-state or transient conditions. The influence of contact force, electric current and ambient temperature on the temperature distribution, has been investigated. A thermal analysis of the different type of the graphite material of fixed electric contact and its influence on contact system temperature rise, has been performed. To validate the three dimensional thermal model, some experimental tests have been done. There is a good correlation between experimental and simulation results.

***Keywords*—**Sliding electric contact, temperature distribution, thermal analysis.

I. Introduction

SLIDING electrical contacts are found in many electromechanical devices, such as relays, switches, current-collection brushes in electrical machines and in special applications, such as pantograph-catenary system or electromagnetic rail launcher. Sliding electrical contacts involve complex phenomenon and their understanding needs large researches to estimate the thermal aspects, the contact resistance, the wear or the material transfer. Temperature rise due to the friction and electrical current may be a major source of sliding electrical contacts deterioration. The contact resistance is largely studied [1], including thermal analysis as in [2]-[5]. Model for temperature estimation of dc-contactors are well developed, as in [6]. The current distribution and thermal effects of the sliding contact arrangement used in high voltage circuit breaker are also studied [7]. It is considered the influence of different factors, such as the size of the contacts and conductors, the structure and resistance of the sliding contact arrangement, the current and temperature distribution and it offers several optimizing measures. Thermal aspects are very important for the sliding contact with lubricants [8], because calculating the contact temperatures between the contacting surfaces makes possible to estimate lubricant degradation and thermal surface failure. It also noticed that for low sliding velocities it can be used the steady state estimation, but for higher sliding velocities there are necessary other methods to estimate the thermal aspects. Specific for the sliding contacts is the difficulty to estimate the temperature variation in the moving contact (because at least one of the contacts is moving). A wireless temperature monitoring with miniature temperature sensors in correlation with the load current provides the means to evaluate physical condition of electrical contacts and detect abnormality and prevent possible disruption of electrical service, [9]. Other thermal measurements possibility is presented in [10], which found the best measurement location as downstream of the nominal contact zone in the moving body. A special area application with sliding electrical contacts is the contact between the pantograph strip and the contact line for the electric vehicles as tramways or electric locomotives, supplied from a pantograph-catenary system, where the contact is realized between two different materials. Mathematical models and simulations for the sliding contact between the pantograph and the contact line are well developed for electrical and mechanical aspects [11], but less with thermal aspects [12]. The sliding electrical contact of pantograph-catenary system in correspondence with the contact force and the electric current is studied in order to estimate the contact resistance [13] and also the damages of the pantograph-catenary system due to the electrical faults in real conditions [14]. The temperature range over the pantograph-catenary system is also studied, as in [15]. Another special application, the electromagnetic launcher, is a short operating time at high currents, pressures and temperatures and the phenomenon occurring at the interface between conductors involved in sliding contacts have been investigated by the introduction of an auxiliary electric network [16]. The control of the interface tribology in sliding electrical contacts requires an understanding of the Joule heating in the vicinity of the interface. In some situations [17], the maximum temperature rise occurs in the bulk of the contacts rather than at the interface and sliding can have a significant effect on the temperature field even for low speed.

This study attempts to achieve and validate a three dimensional thermal model for a sliding contact system with different geometries of fixed and moving contact.

II. Thermal Model

The aim of this study is to develop a three dimensional thermal model of a sliding electric contact system. The basic equation of heat transfer has the following expression for each volume element dV:

$$Q_c = Q_t - Q_r + Q_a \tag{1}$$

The left term of the equation is the heating power from the current flow, Q_c. It is in balance with the heat stored by temporal change of temperature Q_t, the power removed from the element by thermal conduction Q_r, and the thermal power dissipated to the surrounding area by the surface convection,

A. T. Pleşca is with the Gheorghe Asachi Technical University of Iasi, Iasi, IS 700050 Romania (phone: 40-232-278683; fax: 40-232-237627; e-mail: aplesca@ee.tuiasi.ro).

Q_a. For the above thermal power quantities, the following equations can be written:

$$Q_c = \iiint \rho j^2 dV; \quad Q_t = \iiint \gamma c \frac{\partial \theta}{\partial t} dV;$$
$$Q_r = \iiint div(\lambda \cdot grad\theta) dV; \qquad (2)$$
$$Q_a = \iiint k \frac{l}{S}(\theta - \theta_a) dV$$

where:

ρ means the electrical resistivity;
j – current density;
γ – material density;
c – specific heat;
λ – thermal conductivity;
θ – temperature;
θ_a – ambient temperature;
k - convection coefficient;
l – perimeter length of the contacts' cross-section;
S – cross-section of the contacts.

Therefore,

$$\iiint \rho j^2 dV = \iiint \gamma c \frac{\partial \theta}{\partial t} dV - \iiint div(\lambda \cdot grad\theta) dV + \qquad (3)$$
$$+ \iiint k \frac{l}{S}(\theta - \theta_a) dV$$

The material density, specific heat and thermal conductivity do not have an important temperature variation; thus they can be regarded as constants. On the other hand, the electrical resistivity has a significant temperature variation and can be estimated through a parabolic variation or a linear one. In general, the difference between these two types of variation is not so important. For the electrical resistivity we may consider a linear variation with the temperature,

$$\rho = \rho_0 [1 + \alpha(\theta - \theta_a)] \qquad (4)$$

where α is the coefficient of electrical resistivity variation with temperature. Considering the notation:

$$\vartheta = \theta - \theta_a \qquad (5)$$

The following relation is obtained:

$$\iiint \rho_0 (1 + \alpha\vartheta) \frac{i^2}{S^2} dV = \iiint \gamma c \frac{\partial \vartheta}{\partial t} dV - \qquad (6)$$
$$- \iiint div(\lambda \cdot grad\vartheta) dV + \iiint k \frac{l}{S} \vartheta dV$$

Because the sliding electric contact system has not a constant cross section and the physical parameters, especially the electrical resistivity, vary with the temperature, the above equation is a non-linear type with variable coefficients and it demands a numerical procedure to evaluate the temperature distribution. It is desirable to restate the problem by considering various forms of discretization. The discretised form of the problem only requires the solution to be satisfied at a finite number of points in the region; and in the remainder of the region, appropriate interpolations may be used. Thus, this case is reduced to an algebraic form involving only the basic arithmetic operations, which could in turn be solved by numerical methods. These methods have become very accurate and reliable for solving initial and boundary value problems. The basic idea of the finite element method is to discretise the main domain into several subdomains, or finite elements. These elements can be irregular and possess different properties so that they form a basis to discretise complex structures, or structures with mixed material properties.

A three dimensional model for a sliding electric contact system has been developed using specific software like Pro-ENGINEER, which is an parametric, integrated 3D CAD/CAM/CAE solution. Pro-ENGINEER provides a complete set of design, analysis and manufacturing capabilities on one, integral, scalable platform. These required capabilities include solid modelling, surfacing, rendering, data interoperability, routed systems design, simulation, tolerance analysis and tooling design.

An overall view with electric installation including the sliding contact system which has the possibility to use two graphite skate contacts is presented in Fig. 1. The 3D model had taken into consideration all the component parts of the sliding contact system: copper disc, steel pressing piece, gear wheel, main shaft, insulators, graphite skate, spindles, as shown in Fig. 2.

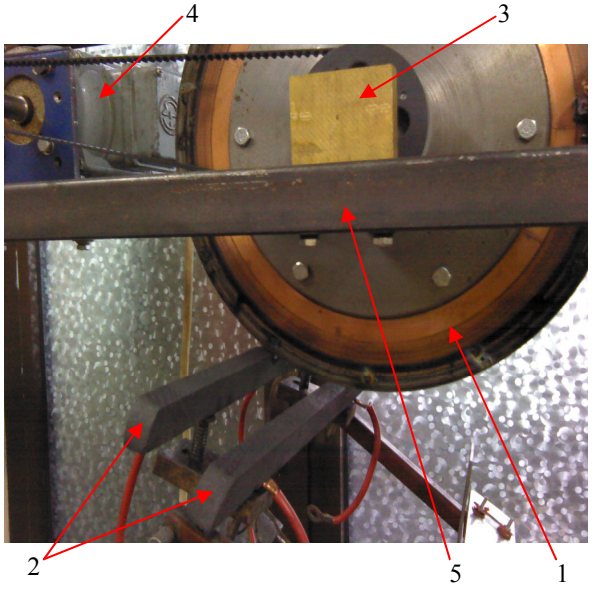

Fig. 1 Sliding system with the following main components: 1 – copper disc; 2 – graphite skate slide contacts; 3 – end insulator; 4 – drive motor; 5 – mechanical structure

III. Thermal Simulations

The Pro-MECHANICA software has been used for all thermal simulations. Pro-MECHANICA uses adaptive p-element technology whereas conventional finite element codes use non-adaptive h-element technology.

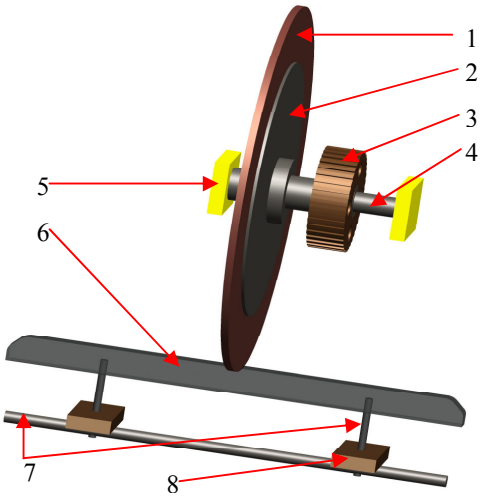

Fig. 2 Thermal model of the copper disc – graphite skate power assembly (1 – copper disc; 2 – steel pressing piece; 3 – gear wheel; 4 – main shaft; 5 – end insulators; 6 – graphite skate; 7 – spindles; 8 - insulators)

The underlying geometry can be followed more precisely. The elements use a polynomial equation to describe the stress shape function, which can vary from 3rd to 9th order. This means that fewer elements are required and they can follow high stress gradients very closely. It also means that an automatic convergence strategy can be employed, whereby the polynomial order of the elements is increased rather than having to re-mesh with smaller elements. Furthermore Pro-MECHANICA has built-in optimisation capabilities, so that designs can be optimised efficiently and automatically.

The material properties of every component part of the sliding contact system, are described in the Table 1, according to Fig. 2. The heat load has been applied on the contact area between copper disc and graphite skate contact. There is a uniform spatial distribution on these elements. The mesh of this 3D sliding contact thermal model has been done using tetrahedron solids element types with the following allowable angle limits (degrees): maximum edge: 170; minimum edge: 5; maximum face: 174.3; minimum face: 5. The maximum aspect ratio was 23.45 and the maximum edge turn (degrees): 95.

The single pass adaptive convergence method to solve the thermal steady-state simulation has been used.

TABLE I
Material Data and Coefficients at 20°C in Correlation with Component Parts from Fig. 2

Parameter	Material			
	Copper (1)	Iron FE40 (2, 3, 4, 7)	Graphite (6)	Insulation material /textolit (5, 8)
γ (kg/m^3)	8900	7190	1900	1350
c (J/kg°C)	385	420.27	1000	733
λ (W/m°C)	385	52.028	160	3.2

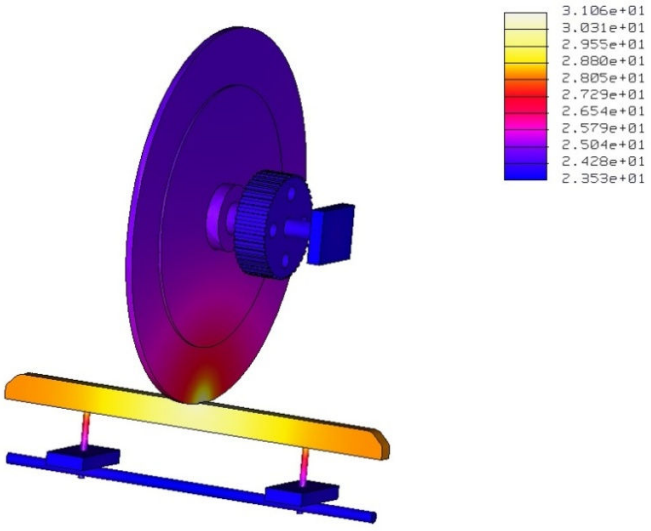

Fig. 3 Temperature distribution on the sliding contact system at current value of 8A and contact force of 10N

The analyzed graphite contact has the following overall dimensions: 400mm long, 18mm wide, 22 mm high. The copper disc has the diameter of 380mm and the thickness about 5mm. The ambient temperature was about 23°C. From experimental tests it was computed the convection coefficient k = 15.3W/m^2°C on the graphite contact. For all metal component parts of the sliding contact system, the convection coefficient was about 19.5W/m^2°C.

It was considered the convection condition like boundary condition for the outer boundaries such as copper disc, steel pressing piece, gear wheel, main shaft, spindles and it has been applied on surfaces with an uniform spatial variation and a bulk temperature of 23ºC. On the insulators, the convection coefficient was about 12W/m^{2}ºC.

Further on, some steady state thermal simulations have been done. The temperature distribution on the sliding contact system is presented in Fig. 3. In Fig. 4 is shown the temperature distribution at a half cross-section through whole copper disc and the rest of the mechanical system. It is to observe the highest temperatures on the contact area between the copper disc and the graphite skate contact.

The copper disc and graphite contact lengthwise temperature distributions for different electric current and contact force value, are presented from Fig. 5 to Fig. 8. Temperature distribution along the radius of the copper disc and length of the graphite contact for different graphite materials and ambient temperature is shown from Fig. 9 to Fig. 12.

IV. Discussion of the Results

In Fig. 5, the temperature distribution along the radius of the copper disc for different values of the test current (4, 8 and 12A), is shown. The contact force has been maintained at the constant value of 10N.

As expected, the higher values of the temperature (θsim_12A) correspond to the higher values of the test current (12A). There is a temperature decreasing as we depart the contact area (x = 0). The temperature decreasing is more pronounced at higher test currents (θsim_12A) than lower current values (θsim_4A). A similar temperature variation lengthwise graphite skate contact, is shown in Fig. 6. The contact force was the same 10N. Also in this case, there is a noticeable decrease in temperature as we depart the contact area (x = 0). After approximately 100mm, the temperature values are almost constant. As expected, at higher current values (12A) there are higher temperature values (θsim_12A). The temperature variation along the radius of the copper disc for different values of the contact force (6, 10 and 15N), is presented in Fig. 7. The electric current had the constant value of 8A. In this case, at lower values of the contact force (6N) there are higher temperatures (θsim_6N). When the contact force has higher values (15N), the temperatures are lower (θsim_15N). This is explained by the fact that a higher contact force, the contact resistance is lower and so, the power loss is lower and finally, the local temperatures are lower. The same temperature distribution lengthwise graphite skate contact, is presented in Fig. 8. It can be noticed that the temperature variation at the same contact force, is insignificant after a distance about 100mm from the contact area.

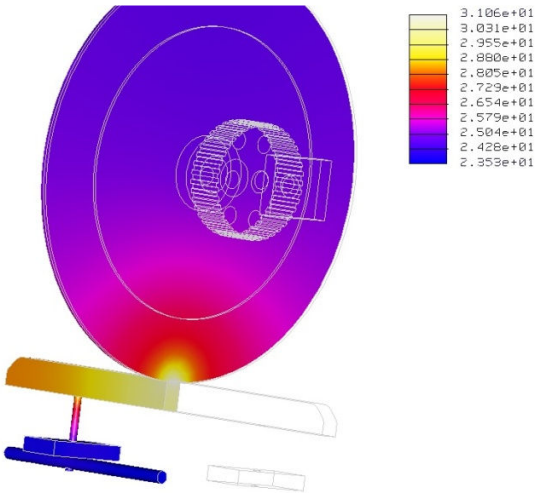

Fig. 4 Temperature distribution on the sliding contact system at current value of 8A and contact force of 10N (50% cross-section through the copper disc and graphite skate)

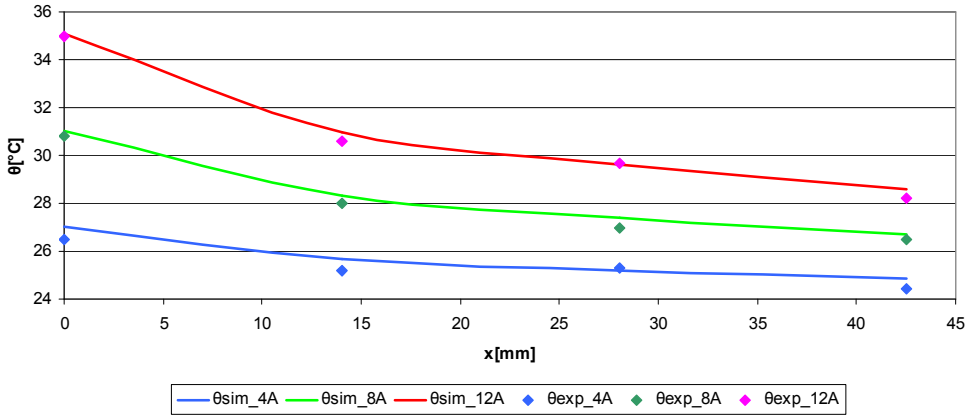

Fig. 5 Temperature variation along the radius of the copper disc for different current values (4, 8 and 12A) and the contact force of 10N. Comparison between simulation values (θsim_4A, θsim_8A and θsim_12A) and experimental results (θexp_4A, θexp_8A and θexp_12A)

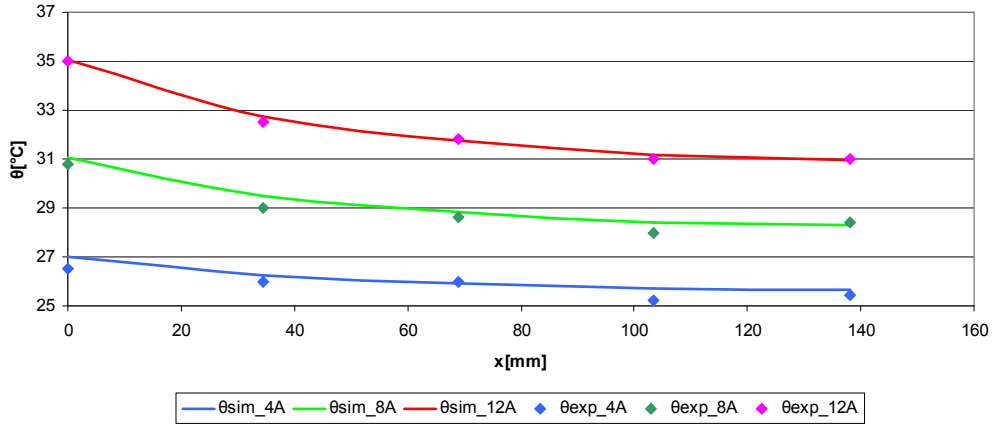

Fig. 6 Temperature variation lengthwise graphite skate contact for different current values (4, 8 and 12A) and the contact force of 10N. Comparison between simulation values (θsim_4A, θsim_8A and θsim_12A) and experimental results (θexp_4A, θexp_8A and θexp_12A)

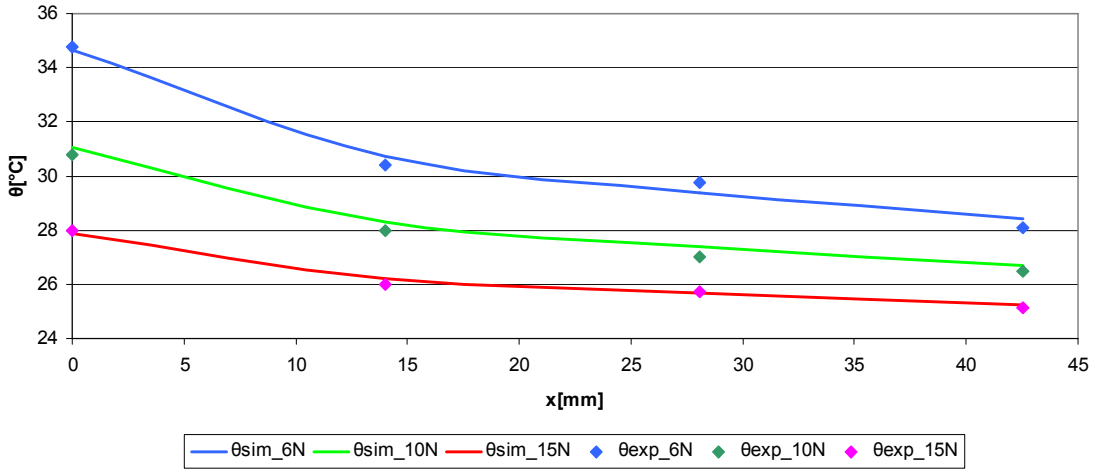

Fig. 7 Temperature variation along the radius of the copper disc for different contact forces (6, 10 and 15N) and the current of 8A. Comparison between simulation values (θsim_6N, θsim_10N and θsim_15N) and experimental results (θexp_6N, θexp_10N and θexp_15N)

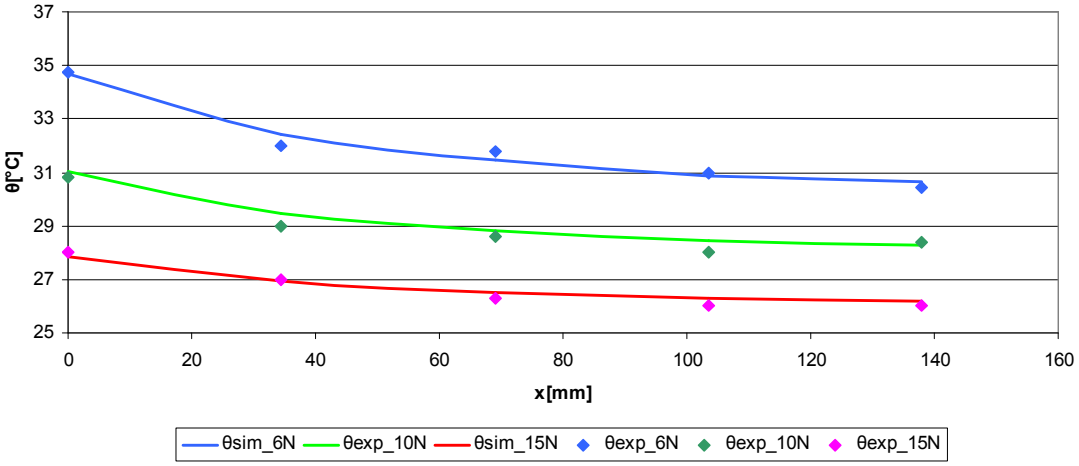

Fig. 8 Temperature variation lengthwise graphite skate contact for different contact forces (6, 10 and 15N) and the current of 8A. Comparison between simulation values (θsim_6N, θsim_10N and θsim_15N) and experimental results (θexp_6N, θexp_10N and θexp_15N)

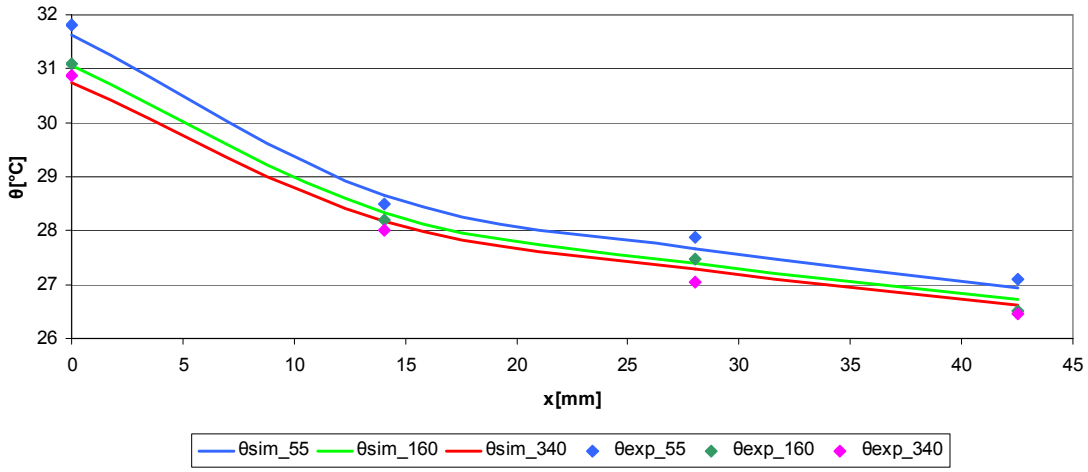

Fig. 9 Temperature variation along the radius of the copper disc for different graphite thermal conductivity values (55, 160 and 340W/mºC) at the current value of 8A and the contact force of 10N. Comparison between simulation values (θsim_55, θsim_160 and θsim_340) and experimental results (θexp_55, θexp_160 and θexp_340)

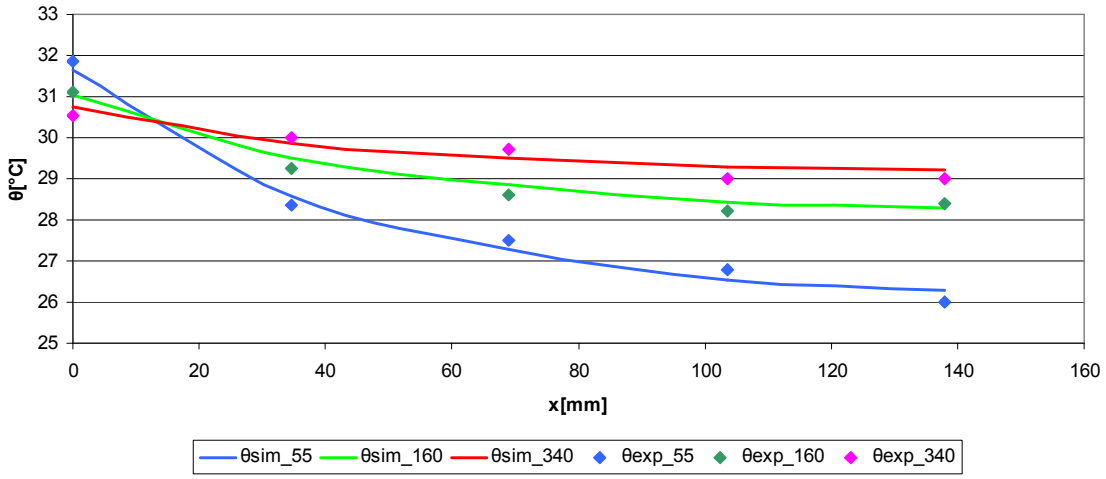

Fig. 10 Temperature variation lengthwise graphite skate contact for different graphite thermal conductivity values (55, 160 and 340W/mºC) at the current value of 8A and the contact force of 10N. Comparison between simulation values (θsim_55, θsim_160 and θsim_340) and experimental results (θexp_55, θexp_160 and θexp_340)

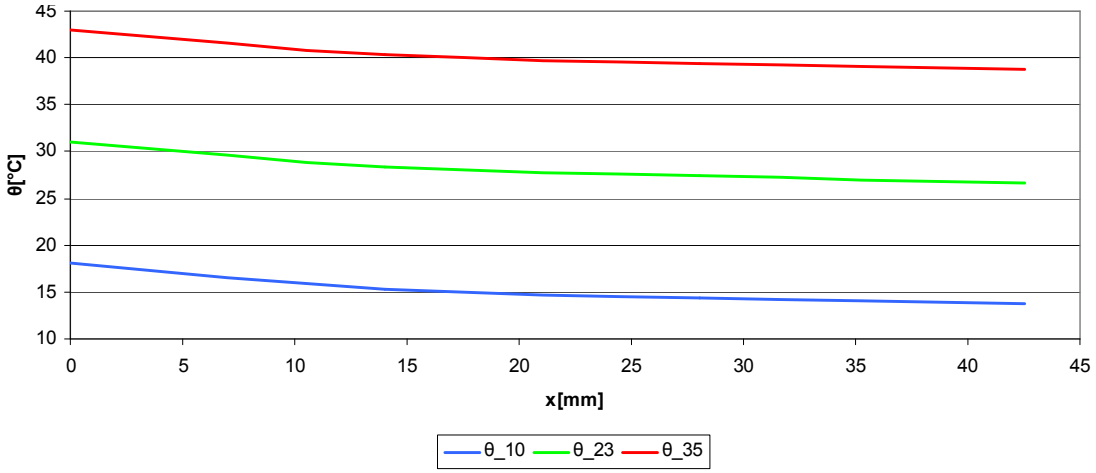

Fig. 11 Temperature variation along the radius of the copper disc for different ambient temperature values (10, 23 and 35ºC) at the current value of 8A and the contact force of 10N

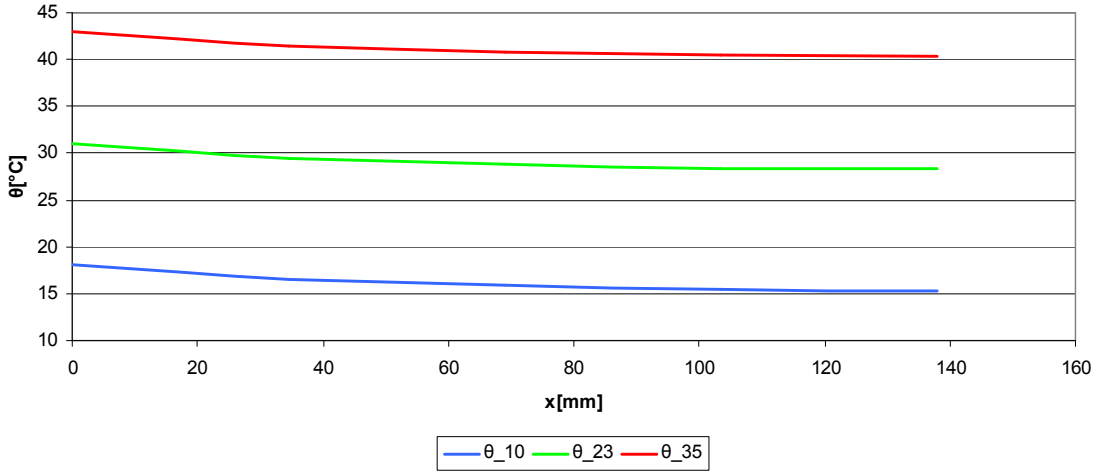

Fig. 12 Temperature variation lengthwise graphite skate contact for different ambient temperature values (10, 23 and 35ºC) at the current value of 8A and the contact force of 10N

In Fig. 9, the temperature variation along the radius of the copper disc for different graphite materials with different thermal conductivity values is presented. The thermal simulations have been performed for a constant current of 8A and a constant contact force of 10N. It has been considered three types of the graphite materials: BGR-3, λ = 55W/mºC; EGR-16, λ = 160W/mºC and MGR-34, λ = 340W/mºC. It can be observed very small differences between temperature variations (θsim_55, θsim_160 and θsim_340). The same case has been analyzed but with the temperature distribution lengthwise the graphite skate contact, Fig. 10. It can be noticed that for the graphite material with higher thermal conductivity (θsim_340), the temperature decreasing is relatively small (under 2ºC); but for the graphite material with lower thermal conductivity (θsim_55), the temperature decreasing is about 6ºC.

The temperature variation along the radius of the copper disc for different ambient temperatures (10, 23 and 35ºC), is depicted in Fig. 11. The test current and the contact force have been maintained at a constant value. It is to observe that the temperature variation curve is translated on vertical direction depending on the temperature ambient values. The same observation is valid in the case of temperature variation lengthwise the graphite skate contact, Fig. 12, for the same different values of the ambient temperatures (θ_10, θ_23 and θ_35). The test current has been considered at the constant value of 8A and also the contact force was maintained at a constant value of 10N.

To validate the simulation results, some experimental tests have been made with the same conditions as in the case of thermal simulations. The electric circuit diagram used for experimental tests is shown in Fig. 13. The main switch K, enables the supply with low-voltage for the auto-transformer ATR, which adjusts the input voltage for the current supply device CS. The high current from CS, flows through the copper disc D and graphite skate contact S.

The current value is measured by an ammeter A, through a current transformer CT. The temperature values are recorded by a compact infrared thermal imaging camera type FLIR E40 with a focal plane array detector of 160 x 120 pixels infrared resolution, temperature range: -20°C to 650°C with ±2% or 2°C accuracy and 0.07°C @ 30°C thermal sensitivity. In fig. 14 and 15, an example of the thermal spectra, in steady-state conditions, of the analyzed sliding contact system for the test current of 8A, contact force of 10N, thermal conductivity of the graphite about 160W/m°C and ambient temperature of 23°C, are presented. The emissivity coefficient was about 0.95. The comparisons between simulation and experimental results are presented from Fig. 5 to Fig. 10. It can be noticed a good correlation between simulation results and experimental values. The differences between the temperature values resulting from experimental tests and those obtained during simulations are due to various factors: measurement errors, thermal model simplifications and mounting test conditions. Nevertheless, the maximum difference between the experimental and simulation results is less than 2.3ºC.

V. Conclusion

The obtained three dimensional thermal models allow analysis of the thermal behaviour of sliding electric contact system. The thermal model provides the sliding contact system temperature distribution at different currents, contact forces, graphite materials and ambient temperature values and could be used as a designing tool for the electric sliding contact systems, especially in the case of electric traction vehicles as tramways and trains. Some experimental tests have been made in order to validate the proposed three dimensional thermal model. There is a good correlation between experimental and simulated results. Using the proposed thermal model, the sliding contact design process can be improved and there is the possibility of obtaining new solutions for an optimal power management of different types of sliding contact systems

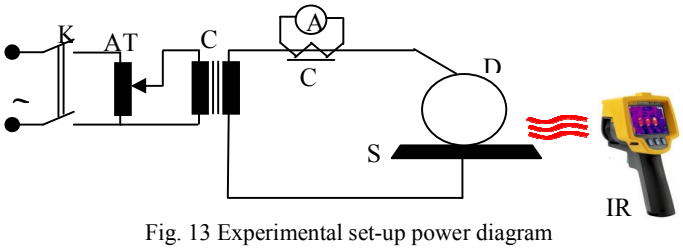

Fig. 13 Experimental set-up power diagram

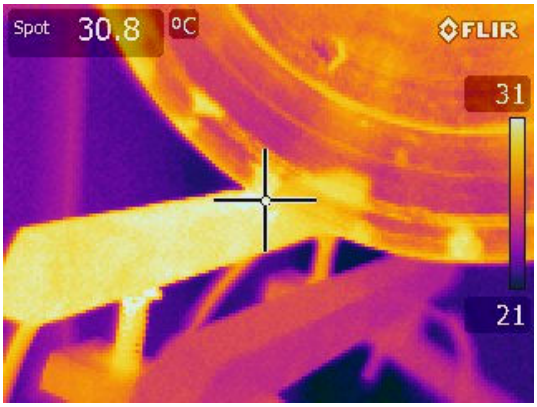

Fig. 14 Thermal spectrum of the sliding contact system for the test current of 8A, contact force of 10N and emissivity coefficient of 0.95

Fig. 15 Thermal spectrum of the sliding contact system for the test current of 8A, contact force of 10N and emissivity coefficient of 0.95 (different angle)

ACKNOWLEDGMENT

This work was supported by CNCSIS – UEFISCDI, project number 610 PNII – CAPACITATI, 2013.

REFERENCES

[1] D. Bansal, Tribological investigation of electrical contacts, Doctoral thesis, Georgia Institute of Technology, 2009, ch.3.
[2] M. Bahrami, J. R. Culham, and M. M. Yovanovich, "Modeling thermal contact resistance: a scale analysis approach," J. of Heat Transf., vol. 126, pp. 896-905, 2004.
[3] M. H. Shojaefard, M. Ghaffarpour, and A. R. Noorpoor, "Thermal contact analysis using identification method," Heat Transf. Engineering, vol. 29, no. 1, pp. 85-96, 2008.
[4] C. Fieberg, and R. Kneer, "Determination of thermal contact resistance from transient temperature measurements," Int. J. of Heat and Mass Transf., vol. 51, pp. 1017–1023, 2008.
[5] A. L. Wang, and J. F. Zhao, "Review of prediction for thermal contact resistance," Science China Technological Sciences, vol. 53, no. 7, pp. 1798-1808, 2010.
[6] M. P. Paisios, C. G. Karagiannopoulos, and P. D. Bourkas, "Model for temperature estimation of dc-contactors with double-break main contacts," Simulation Modelling Practice and Theory, vol. 15, pp. 503 – 512, 2007.
[7] N. Du, Y. G. Guan, W. D. Liu, S. Z. Jin, and M. Collod, "Current distribution and thermal effects analysis on the sliding contact arrangement in circuit breaker," in Proc. of the 11th Int. Conf. on Electrical Machines and Systems, Wuhan, 2008, pp. 447-451.
[8] R. Bosman, and M. B. de Rooij, "Transient thermal effects and heat partition in sliding contacts," J. of Tribology-Trans. of the ASME, vol. 13, no. 2, 2010.
[9] B. H. Chudnovsky, "Electrical contacts condition diagnostics based on wireless temperature monitoring of energized equipment," in Proc. of the 52nd IEEE Holm Conference on Electrical Contacts, Montreal, 2006, pp. 73-80.
[10] B. Vick, and W. C. Schneck, Estimation of the real area of contact in sliding systems using thermal measurements, J. of Tribology-Trans. of the ASME, vol. 133, no. 3, 2011.
[11] A. Collina, and S. Bruni, "Numerical Simulation of Pantograph-Overhead Equipment Interaction," Vehicle System Dynamics, vol. 38, pp. 261-291, 2002.
[12] S. Walters, A. Rachid, and A. Mpanda, "On Modelling and Control of Pantograph Catenary Systems," in Int. Conf. on Pantograph Catenary Interaction Framework for Intelligent Control PACIFIC, Amiens, 2011.
[13] W. Wang, A. Dong, G. Wu, G. Gao, L. Zhou, B. Wang, Y. Cui, D. Liu, D. Li, and T. Li, "Study on characterization of electrical contact between pantograph and catenary," in 57th Holm Conference on Electrical Contacts, Minneapolis, 2011, pp. 1-6.
[14] V. Mihalcea, L. Cantemir, C. G. Cantemir, and G. Chiriac, "The necessity of current collecting study at the pantograph of the electric locomotive in real conditions," Buletinul Institutului Politehnic Iaşi, vol. L (LIV), no. 5, pp. 1159-1164, 2004.
[15] C. Nițucă, L. Cantemir, G. Chiriac, and A. Gheorghiu, "Aspects regarding the influence of the temperature range over the contact line," Buletinul Institutului Politehnic Iaşi, vol. L (LIV), no. 5, pp. 1165-1170, 2004.
[16] A. Musolino, "Electromagnetic analysis in devices with sliding contacts," Int. J. for Computation and Mathematics in Electrical and Electronic Engineering, vol. 20, no. 2, pp. 463-472, 2001.
[17] B. G. Watkins, and J. Streator, "Simulation of thermal effects in stationary and sliding electrical contacts," in Proc. of the STLE/ASME Int. Joint Tribology Conf., Miami, 2008, pp. 661-663

Adrian Pleşca was born in Iasi, Romania, on April 16, 1972. He graduated from the Gheorghe Asachi Technical University of Iaşi and he received the PhD degree in Electrical Engineering in 2001. His employment experience included the Gheorghe Asachi Technical University of Iasi, Power Engineering Department. His special fields of interest included electrical apparatus, special equipment for power semiconductor devices protection and 3D modelling and simulation of the electrical apparatus. Dr. Pleşca received Golden and Silver Medals at World Exhibition of Invention, Research and Industrial Innovation, Brussels, Belgium, EUREKA, 2001, 2004, Special Prize awarded by National Research Council of Thailand for Fundamental Research at The First International Invention's Day Convention, Bangkok, Thailand 2008, Gold Medal at 4th International Warsaw Invention Show 2010, Diploma and Genius Medal at 2nd International Invention Exhibition, Ljubljana, 2010 and Gold Prize at Seoul International Invention Fair, Korea 2011.